Ribose Facilitates Thallium-201 Redistribution in Patients with Coronary Artery Disease

Neal S. Perlmutter, Richard A. Wilson, Debra A. Angello, Robert T. Palac, Jiin Lin, and B. Greg Brown

Division of Cardiology, Oregon Health Sciences University, Portland, Oregon; Portland Veterans Administration Hospital, Portland, Oregon; and Division of Cardiology, University of Washington, Seattle, Washington

To investigate whether i.v. infusion of ribose, an adenine nucleotide precursor, postischemia facilitates thallium-201 (^{201}Tl) redistribution and improves identification of ischemic myocardium in patients with coronary artery disease (CAD), 17 patients underwent two exercise ^{201}Tl stress tests, performed 1-2 wk apart. After immediate postexercise planar imaging, patients received either i.v. ribose (3.3 mg/kg/min × 30 min) or saline as a control. Additional imaging was performed 1 and 4 hr postexercise. Reversible defects were identified by count-profile analysis. Significantly more (nearly twice as many) reversible ^{201}Tl defects were identified on the post-ribose images compared to the post-saline (control) images at both 1 and 4 hr postexercise ($p < 0.001$). Quantitative analyses of the coronary arteriogram was available in 13 patients and confirmed that the additional reversible defects were in myocardial regions supplied by stenosed arteries. We conclude that ribose appears to facilitate ^{201}Tl redistribution in patients with CAD and enhances identification of ischemic myocardium.

J Nucl Med 1991; 32:193–200

Exercise thallium-201 (^{201}Tl) scintigraphy is currently used to assess myocardial viability in patients with coronary artery disease (CAD) (*1*). Reversible ^{201}Tl defects are associated with viable ischemic myocardium, while fixed ^{201}Tl defects have been regarded to represent nonviable, infarcted regions. However, Gutman et al. (*2*) cast doubt on this notion, noting that "fixed" ^{201}Tl defects, observed on 4-hr postexercise planar images, become reversible when patients are imaged 24 hr postexercise. Similar findings during single-photon emission computed tomography (SPECT) imaging have also been reported (*3,4*). "Fixed" ^{201}Tl defects have also disappeared after percutaneous transluminal coronary angioplasty or bypass surgery (*5,6*). Glucose metabolism has also been demonstrated by positron emission tomography (PET) in areas of fixed ^{201}Tl defects (*7*). Thus, myocardial ^{201}Tl redistribution after transient ischemia is sometimes too slow to allow identification of a reversible myocardial defect within the routine (usually 4 hr) imaging period.

Infusion of adenine nucleotide precursors, such as ribose, have been shown to favorably affect myocardial high-energy phosphate stores (*8–12*), regional function (*10,13–15*), and ^{201}Tl kinetics postischemia (*15,16*). Modification of ^{201}Tl clearance in both ischemic and nonischemic myocardial regions has been demonstrated with ribose infusion after transient ischemia in swine (*15,16*), resulting in faster ^{201}Tl redistribution.

This study was designed to determine if i.v. ribose infusion after transient myocardial ischemia can facilitate ^{201}Tl redistribution in patients with CAD, and thus improve the ability to detect jeopardized but viable myocardium.

MATERIALS AND METHODS

Patient Characteristics

Seventeen patients with chronic stable angina were enrolled in the randomized, placebo-controlled crossover trial (Table 1). These patients were referred by their clinicians for noninvasive or invasive evaluation of their chest pain symptoms. The study protocol and informed consent document were approved by the Institutional Review Boards at Oregon Health Sciences University and the Portland Veterans Administration Hospital. All patients either had known CAD (as documented by coronary angiography, n = 14) or an extremely high likelihood of CAD (as evidenced by classic angina and electrocardiographic ST segment depression of at least 2.0 mm during an episode of chest pain, n = 3). Patients with unstable angina, diabetes mellitus, inability to exercise, atypical chest pain, or no angina were excluded from the trial. Each patient underwent two separate ^{201}Tl exercise tests, performed 1-2 wk apart. Chronic anti-anginal medications were not discontinued prior to exercise testing. The severity of anginal symptoms was determined according to the Canadian Cardiovascular Society classification (*17*). No medication changes were permitted between the two tests, and no patient experienced an interval change in cardiac symptoms or electrocardiogram.

Exercise Testing and ^{201}Tl Imaging

The study protocol is shown in Figure 1. Intravenous catheters were placed in the left arm for injection of ^{201}Tl and ribose/normal saline and in the right arm for blood drawing.

Received Apr. 19, 1990; revision accepted Aug. 2, 1990.

For reprints contact: Richard A. Wilson, MD, Div. of Cardiology, L-462, Oregon Health Sciences Univ., 3181 S.W. Sam Jackson Park Rd., Portland, OR 97201-3098.

TABLE 1
Patient Characteristics

Age (yr)	65.8 ± 12.4
Sex	14 male, 3 female
Prior coronary arteriography	14 (82%)
1 vessel disease	2 (14%)
2 vessel disease	4 (29%)
3 vessel disease	7 (50%)
Left main + right coronary disease	1 (7%)
Q-wave myocardial infarction with wall motion abnormality	4 (24%)
Prior coronary bypass surgery	3 (18%)
Anti-anginal medications	
Beta blockers	11 (65%)
Calcium channel blockers	15 (88%)
Nitrates	8 (47%)
Canadian Cardiovascular Society grading for effort angina	
I	6 (35%)
II	7 (41%)
III	4 (24%)
IV	0 (0%)

An exercise protocol was selected appropriate to the patient's exercise capacity (either Bruce or modified Bruce protocol). Treadmill exercise was performed until angina or other limiting symptoms occurred. At that time, ~74 mBq (2.0 mCi) of ^{201}Tl were injected intravenously and exercise continued for an additional 60 sec. Within 3 min after cessation of exercise, planar ^{201}Tl myocardial imaging was begun. Images were acquired with a standard gamma scintillation camera with a low-energy all-purpose collimator. Images in each sequence were obtained in the anteroposterior, 45° left anterior oblique, and 70° left anterior oblique projections. Each projection was acquired over 10 min (resulting in a total imaging time of ~30 min for each sequence).

After immediate postexercise imaging was completed, a 30-min infusion of either ribose (3.3 mg/kg/min, 10% solution) or normal saline (equivalent volume) was given through the i.v. catheter in the left arm. Immediately after this infusion was completed, ^{201}Tl imaging was again performed. A final sequence of ^{201}Tl images was obtained at 4 hr postexercise.

During the second exercise test, performed 1-2 wk later, patients were exercised according to the same protocol and exercise was carried out to the same heart rate × blood pressure product achieved on the first test. The second test was stopped before this time, however, if severe angina or other limiting symptoms occurred. After immediate postexercise imaging, patients received whichever infusion had not been administered previously. The study protocol was conducted in an otherwise identical manner in both exercise test and imaging sessions.

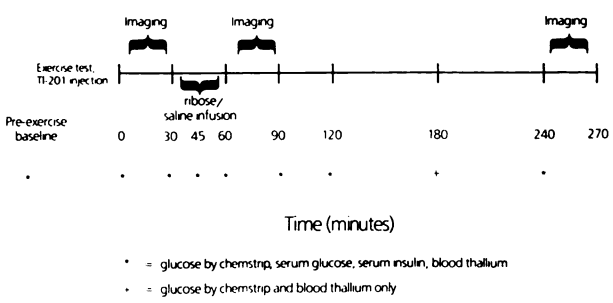

FIGURE 1
Study protocol.

The order of ribose or saline administration was randomized between patients in order to avoid the influence of any possible training effect. Patients were unaware of which infusion was being administered during each test.

Since ribose has been shown to decrease blood glucose levels in man (*18*), glucose was monitored by glucometer-measured chemstrips pre-exercise, pre-infusion, at mid-infusion, at end-infusion, and at 30, 60, 120, and 180 min after infusion. Blood was also obtained at these times for determination of serum glucose, serum insulin, and blood thallium activity (although serum glucose and insulin measurements were not performed 120 min postinfusion).

Patients were instructed not to eat during the entire imaging period (beginning at midnight on the night before each exercise test), since eating has been shown to attenuate ^{201}Tl redistribution (*19,20*).

Thallium-201 Image Analysis and Interpretation

Background subtracted images were interpreted without knowledge of patient identity, catheterization findings, or intervention received. A computer-assisted image processing algorithm generated relative ^{201}Tl activity circumferential count profile analyses for immediate postexercise and delayed ^{201}Tl images (*20,21*). Initial ^{201}Tl defects were identified as regions with relative ^{201}Tl activity less than two standard deviations below a mean value for a group of normal patients (*21*). The circumferential count profile analyses for initial and delayed images were normalized to the peak myocardial activity within that image. Reversible defects were then identified by observing a >12% relative increase in ^{201}Tl activity in the region of the defect between initial and delayed image profiles, as seen over >18° of the arc (*20,21*). All initial ^{201}Tl defects not meeting these redistribution criteria were interpreted as fixed ^{201}Tl defects. To determine if initial postexercise ^{201}Tl defects were similar on the ribose and saline control tests, the defects on the initial postexercise images were quantitated as the percent decrease in ^{201}Tl activity relative to the region with maximal ^{201}Tl activity.

Thallium-201 myocardial clearance profiles were also generated between immediate and 1-hr postexercise and between immediate and 4-hr postexercise images. In each projection of the imaging sequence, nonischemic regional ^{201}Tl myocardial clearance was recorded at the point of maximum relative ^{201}Tl activity. Within each reversible defect, corresponding ischemic regional ^{201}Tl clearance was recorded at the point of maximum activity difference between initial and delayed images (*21*).

Coronary Arteriography and Interpretation

Selective coronary arteriography was performed for clinical indications in 14 of the 17 patients. While blinded to the patient's identity and scintigraphic data, individual maps were made showing the relative size and distribution of each patient's major coronary arteries and the location and severity

of all coronary stenoses. All narrowings that appeared at least 20% by visual interpretation were analyzed using the computer-assisted method described previously (*22*). Stenoses which were quantitatively analyzed were prospectively localized to one or more of the myocardial regions shown in Figure 2. Lesions with ≥50% diameter luminal narrowing were considered significant (*23*).

Biplane contrast left ventriculography was performed in 30° right anterior and 60° left anterior oblique views. Regional wall motion was assessed qualitatively by the consensus of two observers who were blinded to the results of the ^{201}Tl tests. Regional wall motion was graded as normal, hypokinetic, akinetic, or dyskinetic in the anterior, apical, inferior, septal, and posterolateral walls. Regions of wall motion from left ventriculography were paired with the seven regions from the ^{201}Tl imaging (in parentheses) as follows: anterior (anterior, anterolateral), apical (apex), inferior (inferior, inferoposterior), septal (septal), and posterolateral.

One patient, who had arteriography performed at an outside institution, did not have cineangiograms available for quantitative analysis (although three-vessel coronary disease was described by report). The median interval between cardiac catheterization and completion of both thallium studies was 5 wk. No patient had an interval change in cardiac symptoms or electrocardiogram between the catheterization and ^{201}Tl studies.

Blood ^{201}Tl Activity

Samples for whole blood and plasma ^{201}Tl activity were counted by a standard gamma well counter, and counts per gram of blood or plasma were calculated after background subtraction. Counts per gram were normalized to the initial (30 min postinjection) value.

Statistical Analysis

The number of reversible defects between ribose and saline interventions was compared by McNemar's test (paired chi-square analysis). Initial postexercise ^{201}Tl defect severity and ^{201}Tl myocardial clearance, in both ischemic and nonischemic regions, were compared between ribose and saline interventions by paired t-test.

Exercise test characteristics were compared between ribose and saline interventions by paired t-test. Heart rate, blood pressure, and double product (heart rate × systolic pressure) as well as glucose, insulin, blood and plasma ^{201}Tl levels were compared between interventions over time by analysis of variance with range testing when appropriate. A p value of <0.05 was considered to be significant. Data are expressed as mean ± s.d.

FIGURE 2
Myocardial perfusion regions as seen in the various imaging projections. Seven perfusion regions were defined for each patient in the study. AP = anteroposterior, 45 LAO = 45° left anterior oblique, 70 LAO = 70° left anterior oblique. ANT = anterior, AL = anterolateral, AP = apical, INF = inferior, INFPOST = inferoposterior, PL = posterolateral, and SEP = septal.

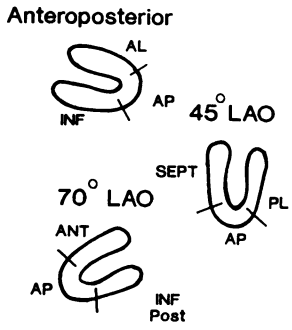

RESULTS

Exercise Testing

Maximum heart rate (114 ± 21 and 117 ± 24 bpm), blood pressure (160 ± 21 and 157 ± 24 mmHg), and double product (18.2 ± 4.4 × 10^3 and 18.3 ± 4.8 × 10^3 bpm × mmHg) were not significantly different between ribose and saline exercise tests, respectively. There was also no significant difference between the tests in the frequency of angina or electrocardiographic ischemic changes seen at peak exercise.

Thallium-201 Scintigraphy and Coronary Arteriography

Table 2 illustrates the results of ^{201}Tl scintigraphy and quantitative coronary arteriography for each patient in the study. Reversible ^{201}Tl defects that would be predicted based on the quantitative coronary arteriography are shown in a column adjacent to the reversible ^{201}Tl defects actually identified on the 1- and 4-hr postexercise images. Of the 75 observed reversible ^{201}Tl defects, the relative ^{201}Tl activity within the initial postexercise defect was 66.2% ± 11.1% for the ribose test and 66.3% ± 11.1% for the saline test, p = 0.84.

Ribose appears to facilitate ^{201}Tl redistribution at 1 hr postexercise (Fig. 3A). This facilitation of redistribution is evident even at the conventional 4-hr imaging time (Fig. 3B). Fig. 4 shows an example of more definite ^{201}Tl redistribution after ribose infusion. At either imaging time, nearly twice the number of reversible defects were identified after ribose infusion, as compared to saline. In 13 of 17 patients, imaging after ribose infusion identified additional reversible defects, as compared to saline.

Similar results were obtained in the subset of 13 patients who underwent quantitative coronary arteriographic analysis (Fig. 5). One-hour and 4-hr ribose images showed more reversible ^{201}Tl defects than did the 1-hr and 4-hr saline images. One or more coronary lesions were prospectively assigned to their corresponding ^{201}Tl scintigraphic regions in each major coronary distribution. Seven of these 13 patients had at least one additional myocardial region supplied by a stenotic artery and was identified as a reversible defect with imaging after ribose infusion, as compared to saline 4-hr postexercise images.

There was no significant difference in the angiographic severity (as defined by % diameter stenosis) among the three major coronary arteries (left anterior descending, 72% ± 18%; circumflex, 74% ± 20%; and right coronary, 84% ± 18%; p = ns). However, reversible ^{201}Tl defects were identified more frequently in the territory of the left anterior descending artery compared to the circumflex artery on the 4-hr saline images (82% versus 30%, respectively, $p < 0.05$) but not on the 4-hr ribose images (91% versus 80%, respectively, p = ns). In 51/54 (94%) of regions with reversible ^{201}Tl defects,

TABLE 2
Thallium-201 Scintigraphy and Coronary Arteriography Results

Pt.	Age (yr) and sex	ECG Qs + WMA	s/p CABG	No. of DV	Coronary stenoses ≥50% (% diameter) LAD	CX	RCA	LM	Predicted ^{201}Tl Defects	Observed ^{201}Tl reversible defects: 1-hr images Saline	1-hr images Ribose	4-hr images Saline	4-hr images Ribose
Patients Undergoing Quantitative Coronary Angiography													
1	58 M	–	–	2	100	–	100	–	ANT, AL, SEP, AP INF, INFPOST	ANT AP(2)	INF	ANT, AP, SEP INF	AP, SEPAL, SEP, AP INF
2	45 M	+	+	3	68	100	100	–	ANT, AL, SEP, AP PL, INF, INFPOST	AL	AL, INF	ANT, AL	ANT, AL, SEP PL, INF
3	87 F	–	–	3	55	76	100	–	ANT, AL, PL INF, INFPOST	—	ANT, AL, INF INFPOST	PL, INFPOST	ANT, AL, PL INFPOST
4	80 M	–	–	2	59	78	n/a	–	ANT, AL, SEP, AP INF, PL, INFPOST	AL, SEP	AL, SEP AP, INF	AL, AP, PL	AL, AP, PL
5	57 M	+	–	1	62	–	–	–	ANT, AL, AP	—	AP	AP	AL, AP
6	78 M	–	–	3	56	57	66	56	ANT, AL, SEP, AP PL, INF, INFPOST	AL, SEP	ANT, AL AP(2) SEP, INFPOST	AL, INF	ANT, AP, PL
7	57 M	–	–	1	–	50	–	–	PL	—	—	—	—
8	57 M	+	+	3	72	100	100	–	ANT, AL, SEP, PL INF, INFPOST	—	AL, SEP	PL, SEP	ANT, PL, SEP
9	70 M	–	–	3	65	100	81	–	ANT, AL, SEP, AP PL, INF, INFPOST	AP, INF INFPOST	AL, AP(2) PL, INF	ANT, AL, INF INFPOST	ANT, AP(3) INF, INFPOST
10	64 M	+	–	1	100	–	–	–	ANT, AL, SEP, AP	AP(2)	—	ANT, SEP, AP	ANT
11	66 F	–	–	2	–	50	73	–	PL, INF, AP	PL	PL, AP	—	PL, AP
12	67 M	–	+	2	100	66	n/a	–	ANT, AL, INF, PL INFPOST, AP	—	AL, INF, AP	—	PL, AP
13	62 M	–	–	3	59	59	55	–	ANT, AL, SEP, AP PL, INF, INFPOST	AL, SEP AP	ANT, SEP, AP INF, INFPOST	AP	AL, AP(2), SEP, INF, PL, INFPOST
Patients Not Receiving Quantitative Coronary Angiography													
14	66 M	–	–							ANT, SEP	ANT, AL, SEP AP, PL, INF	ANT, AP(3) PL, INF, INFPOST	ANT, AL, SEP, AP(3) PL, INF, INFPOST
15	89 M	–	–							—	SEP, AP	AP	SEP, AP, INF
16	47 M	–	–							SEP, AP PL	SEP, AP	AL, AP SEP, INF	AL, SEP, AP, INF
17	68 F	–	–	3	+	+	+	–2*	ANT, AL, SEP, AP PL, INF, INFPOST	—	AL, AP, PL	SEP	ANT, SEP, INFPOST

CABG = coronary artery bypass grafting, CX = circumflex coronary artery and its branches, DV = diseased vessels, ECG = electrocardiogram, LAD = left anterior descending and its branches, LM = left main, n/a = not applicable, since coronary system is left dominant, RCA = right coronary artery and its branches, and WMA = wall motion abnormality. Other abbreviations as in Figure 2.

* Three-vessel disease described by report; films not available for quantitative analysis.

AP(2) = reversible defects identified in apical regions on two different image projections.

the wall motion was either normal [n = 38 (70%)] or hypokinetic [n = 12 (22%)]. In only four (7%) regions of ^{201}Tl reversibility were akinetic walls identified. No reversible ^{201}Tl defects were associated with dyskinetic walls.

The detection of *initial* ^{201}Tl defects in the territories of individual coronary arteries with significant stenoses were also not significantly different for either the saline or ribose tests [left anterior descending 11/11 (100%) and 11/11 (100%), right coronary artery 7/8 (88%) and 8/8 (100%), and circumflex 8/10 (80%) and 9/10 (90%), respectively].

Serum glucose levels fell significantly only at 30 min after ribose infusion (100 ± 12 to 88 ± 15 mg/dl) as compared to saline (107 ± 16 to 102 ± 11 mg/dl, respectively, $p < 0.05$). Although one patient had a fall in serum glucose to 55 mg/dl, no patient developed symptomatic hypoglycemia or required treatment. No adverse reactions were noted during ribose infusion. Serum insulin levels did not change significantly.

Figure 6 illustrates whole blood ^{201}Tl levels over time. No significant differences are noted in whole blood ^{201}Tl activity between the ribose and saline tests. In a subset of nine patients, plasma ^{201}Tl values were also not significantly different between ribose and saline tests.

Table 3 describes ^{201}Tl clearance from the myocardium. Ribose appears to accelerate ^{201}Tl clearance from the normal (nonischemic) regions, as compared to saline. This difference is first apparent at 1 hr postexercise, and becomes more prominent at 4 hr postexercise. Ischemic regional ^{201}Tl clearance appears slightly slower immediately after ribose infusion, as compared to saline; no significant difference is seen at 4 hr postexercise.

FIGURE 3
(A) Number of reversible defects identified on 1-hr postexercise images (performed immediately after infusion of either ribose or saline). Seven scintigraphic perfusion regions were included for each patient in the study since the apex was only counted once. (B) Number of reversible defects identified on 4-hr postexercise images. At both 1 and 4 hr post-exercise images. At both 1 and 4 hr postexercise, a significantly greater number of reversible defects is seen after ribose infusion. +RD = reversible defect present and −RD = reversible defect absent.

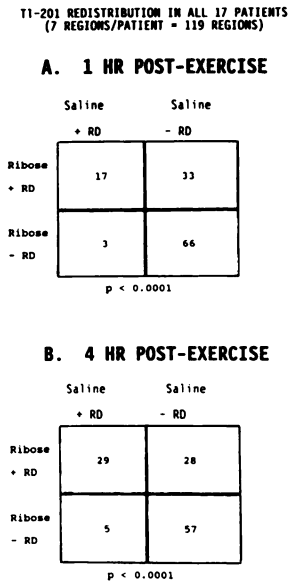

DISCUSSION

This pilot study demonstrates that ribose infusion postischemia can facilitate ^{201}Tl redistribution in patients with CAD and thereby enhance the identification of ischemic myocardium during ^{201}Tl imaging.

Fixed ^{201}Tl defects, observed 3-4 hr postexercise, previously were felt to represent nonviable, infarcted myocardium. These defects have been noted to become reversible when further delayed (i.e., 8–24-hr postexercise) imaging is performed (*2–4*). Myocardial ^{201}Tl redistribution after transient ischemia may simply be too slow, in some cases, to allow identification of a reversible myocardial defect within the routine imaging period. Interventions that facilitate ^{201}Tl redistribution, such as ribose infusion post-ischemia, attempt to circumvent this difficulty, and thereby improve the sensitivity of the ^{201}Tl imaging technique for detecting jeopardized but viable myocardium.

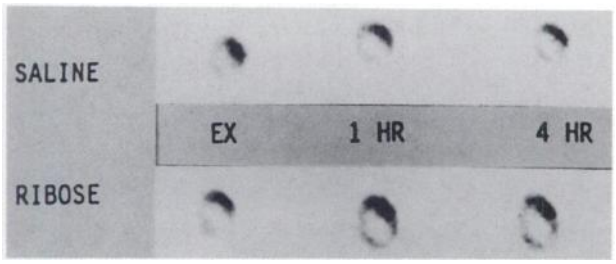

FIGURE 4
Thallium-201 scintigraphic images of Patient 3. From left to right, anteroposterior images obtained immediately postexercise, immediately after saline/ribose infusion (1 hr post-exercise), and delayed images (4 hr postexercise). Reversible defects are identified in the distal anterolateral and inferior regions on the 1-hr and 4-hr ribose images but not on the saline images.

Possible Mechanisms of Action

The mechanism by which ribose influences ^{201}Tl myocardial clearance is not known. Previous studies suggest that coronary blood flow is not the only determinant of postischemic ^{201}Tl redistribution (*15,16,24–28*). Ribose appeared to increase ^{201}Tl myocardial clearance in nonischemic regions on 1- and 4-hr postexercise images, which is likely responsible for the more frequent ^{201}Tl redistribution we observed. In the transiently ischemic regions, ribose appeared to slow ^{201}Tl myocardial clearance at 1 hr but not at 4 hr. The effect of ribose in accelerating ^{201}Tl myocardial clearance in normally perfused regions in this study is similar to the effect observed in animal models in our laboratory (*15, 16*). However, the transiently ischemic regions showed a slower ^{201}Tl myocardial clearance rate at 1 hr in this study whereas the animal studies showed a faster clearance rate from the transiently ischemic region. This discrepancy may be related to differences in the metabolic and physiologic state of the ischemic myocardium between the animal and human studies. There was no significant difference in blood or plasma ^{201}Tl activity between the two protocols to explain the more frequent ^{201}Tl redistribution induced by ribose. Previous studies have shown that infusions of glucose-insulin-potassium (*27,28*) or eating (*19,20*) can attenuate ^{201}Tl redistribution. Ribose may have altered ^{201}Tl kinetics by affecting glycolysis and high-energy phosphate availability (*8–12*) for membrane cation transport (*29,30*).

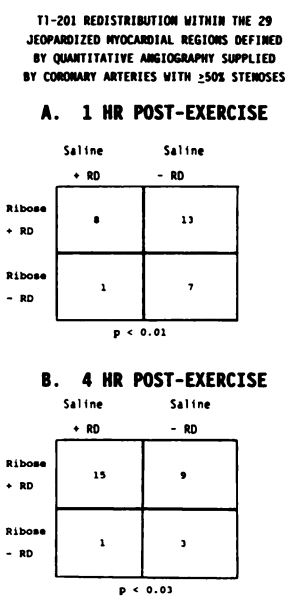

FIGURE 5
Scintigraphic results of the 13 patients who underwent quantitative coronary arteriographic analysis. One or more coronary lesions were prospectively assigned to their corresponding ^{201}Tl scintigraphic regions in each major coronary distribution. Angiography revealed 29 left ventricular myocardial territories supplied by arteries with at least one ≥50% diameter stenosis. (A) Number of myocardial angiographic territories containing a reversible defect that were identified on 1-hr postexercise images (performed immediately after infusion of either ribose or saline). (B) Number of myocardial angiographic territories containing a reversible defect that were identified on 4-hr postexercise images. At both 1 and 4 hr postexercise, a significantly greater number of reversible defects is seen after ribose infusion.

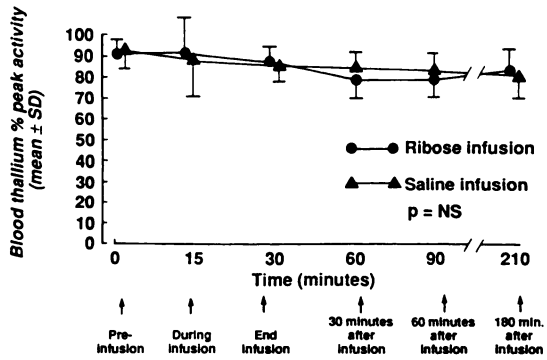

FIGURE 6
Blood ^{201}Tl activity over time during the study protocol. No significant change is seen after ribose infusion as compared to saline. Counts per gram of blood were normalized to the initial (30 min postinjection) blood sample.

Clinical Utility

Detection of *reversible* ^{201}Tl defects using planar imaging appears to be clinically useful for predicting future cardiac events (*31–41*). Thallium-201 imaging, performed after postischemic ribose infusion, predicted the presence of ^{201}Tl redistribution (i.e., jeopardized but viable myocardium) within regions of specific coronary stenoses better than traditional ^{201}Tl imaging techniques, and in most cases, identified new potential areas requiring revascularization. Previous studies have related the severity of the coronary stenosis to the presence or absence of a reversible ^{201}Tl defect (*2,4,42*). In our patients, 76% of the significant stenoses identified had diameter narrowings in the 50%-80% range. In these cases, clinicians may wish to request physiologic testing (such as ^{201}Tl imaging) in order to decide whether revascularization is appropriate. Dilatation of nonobstructive stenoses can clearly lead to clinical harm (*43*).

Although no "gold standard" for myocardial viability exists (short of pathologic examination), viability is usually presumed if normal wall motion is present. Also, hypokinetic walls and even some akinetic walls contain viable myocardium (*6,7,44–48*) whose regional wall motion may improve after revascularization (*44, 46–48*). Therefore, it is likely that the observed ^{201}Tl redistribution did occur in viable myocardial regions.

Study Limitations

Planar imaging, compared to SPECT, may be inferior for lesion detection of left anterior descending and circumflex artery stenoses or certain patient subgroups (*49–53*). This study also demonstrated a low sensitivity of reversible defects (but not initial postexercise defects) for detecting circumflex lesions but not left anterior descending lesions. Nevertheless, planar imaging has been shown to be predictive of future cardiac events (*31–41*). Further studies will be needed to determine the efficacy of ribose infusion after ^{201}Tl tomographic imaging. Previous studies have suggested that 24-hr delayed imaging is superior to 4-hr delayed imaging for detecting reversible ^{201}Tl defects (*2–4*). Therefore, 4-hr post-ribose imaging will need to be compared with 24-hr delayed imaging to determine if 24-hr imaging is superior to 4-hr post-ribose imaging in certain clinical conditions. Similarly, the effect of ribose infusion on ^{201}Tl redistribution with dipyridamole imaging may be different.

Percent stenosis may not always be the most appropriate way to define flow limitation in human atherosclerosis (*54*). However, it is the definition upon which most coronary revascularization decisions are made, and it can be applied to segments in both the proximal and distal coronary arterial tree. Patients were studied while they continued to take anti-anginal medications. No data are available in this study concerning the effect of ribose on ^{201}Tl kinetics in patients not on anti-anginal therapy. No patient experienced symptomatic hypoglycemia. However, the fact that serum glucose fell significantly after ribose infusion is of concern. Serial glucose monitoring will likely continue to be required until further experience is gained with this agent.

Although the number of patients in this study was small, each patient did serve as his own control, allowing direct comparison of the effects of ribose in each stenotic coronary segment. Larger numbers of patients will be required in order to more accurately determine the sensitivity and specificity of ^{201}Tl imaging after postischemic ribose infusion for detecting individual coronary stenoses.

ACKNOWLEDGMENTS

The authors acknowledge the expert technical assistance of Jerry Jarboe, Marina McNeil, Abbe Miley, Ray Wiegner, John Hanada, Drew Poulin, and Mary Joyce, the generous donation of ^{201}Tl by the Diagnostic Imaging Division, Dupont Company, and the excellent secretarial assistance of John Davis.

This study was supported by a grant from the Medical

TABLE 3
% ^{201}Tl Myocardial Clearance in All 17 Patients

	1-hr postexercise images (n = 53)			4-hr postexercise images (n = 54)		
	Ribose	Saline	p value	Ribose	Saline	p value
Normal regions	24.3 ± 16.1	19.8 ± 14.1	0.0001	48.6 ± 12.7	40.2 ± 17.4	0.00004
Ischemic regions	11.0 ± 13.3	13.5 ± 12.9	0.02	32.3 ± 16.4	31.5 ± 18.0	ns

Research Foundation of Oregon and by the National Institutes of Health institutional training grant (5T32-HL07596-03).

REFERENCES

1. Pohost GM, Zir LM, Moore RH, McKusick KA, Guiney TE, Beller GA. Differentiation of transiently ischemic from infarcted myocardium by serial imaging after a single dose of thallium-201. *Circulation* 1977;55:294–302.
2. Gutman J, Berman DS, Freeman M, et al. Time to completed redistribution of thallium-201 in exercise myocardial scintigraphy: relationship to the degree of coronary artery stenosis. *Am Heart J* 1983;106:989–995.
3. Cloninger KG, DePuey EG, Garcia EV, et al. Incomplete redistribution in delayed thallium-201 single photon emission computed tomographic (SPECT) images: an overestimation of myocardial scarring. *J Am Coll Cardiol* 1988;12:955–963.
4. Kiat H, Berman DS, Maddahi J, et al. Late reversibility of tomographic myocardial thallium-201 defects: an accurate marker of myocardial viability. *J Am Coll Cardiol* 1988;12:1456–1463.
5. Liu P, Kiess MC, Okada RD, et al. The persistent defect on exercise thallium imaging and its fate after myocardial revascularization: does it represent scar or ischemia? *Am Heart J* 1985;110:996–1001.
6. Gibson RS, Watson DD, Taylor GJ, et al. Prospective assessment of regional myocardial perfusion before and after coronary revascularization surgery by quantitative thallium-201 scintigraphy. *J Am Coll Cardiol* 1983;1:804–815.
7. Brunken R, Schwaiger M, Grover-McKay M, Phelps ME, Tillisch J, Schelbert HR. Positron emission tomography detects tissue metabolic activity in myocardial segments with persistent thallium perfusion defects. *J Am Coll Cardiol* 1987;10:557–567.
8. Zimmer HG, Gerlack E. Stimulation of myocardial adenine nucleotide biosynthesis by pentoses and pentitols. *Pflugers Arch* 1978;376:223–227.
9. Zimmer HG, Trendelenberg C, Kammermeier H, Gerlack E. De novo synthesis of myocardial adenine nucleotides in the rat. *Circ Res* 1973;32:635–642.
10. Zimmer HG, Ibel H. Effects of ribose on cardiac metabolism and function in isoproterenol-treated rats. *Am J Physiol* 1983;245:H880–H886.
11. Mauser M, Hoffmeister HM, Nienaber C, Schaper W. Influence of ribose, adenosine, and "AICAR" on the rate of myocardial adenosine triphosphate synthesis during reperfusion after coronary artery occlusion in the dog. *Circ Res* 1985;56:220–230.
12. Seiss M, Delabar U, Seifart HJ. Cardiac synthesis and degradation of pyridine nucleotides and the level of energy-rich phosphates influenced by various precursors. *Adv Myocardial* 1983;4:287–308.
13. Haas GS, DeBoer LWV, O'Keefe DO, et al. Reduction of postischemic myocardial dysfunction by substrate repletion during reperfusion. *Circulation* 1984;70(suppl I):I-65–I-74.
14. Pasque MK, Spray TL, Pellom GL, et al. Ribose-enhanced myocardial recovery following ischemia in the isolated working rat heart. *J Thorac Cardiovasc Surg* 1982;83:390–398.
15. Angello DA, Wilson RA, Gee D. Ribose improves postischemic myocardial function and thallium-201 redistribution [Abstract]. *Circulation* 1987;76(suppl IV):65.
16. Angello DA, Wilson RA, Gee D. Effect of ribose on postischemic Tl-201 kinetics. *J Nucl Med* 1988;29:1943–1950.
17. Campeau L. Letter to the Editor. *Circulation* 1976;54:522.
18. Wyngaarden JB, Segal S, Foley JB. Physiological disposition and metabolic fate of infused pentoses in man. *J Clin Invest* 1957;36:1395–1407.
19. Wilson RA, Sullivan PF, Okada RD, et al. The effect of eating on thallium myocardial imaging. *Chest* 1986;89:195–198.
20. Angello DA, Wilson RA, Palac RT. Effect of eating on thallium-201 myocardial redistribution after myocardial ischemia. *Am J Cardiol* 1987;60:528–533.
21. Maddahi J, Garcia EV, Berman DS, Waxman A, Swan HJC, Forrester J. Improved noninvasive assessment or coronary artery disease by quantitative analysis of regional stress myocardial distribution and washout of thallium-201. *Circulation* 1981;64:924–935.
22. Brown BG, Bolson E, Frimer M, Dodge HT. Quantitative coronary arteriography. Estimation of dimensions, hemodynamic resistance, and atheroma mass of coronary artery lesions using the arteriogram and digital computation. *Circulation* 1977;55:329–337.
23. Gould KL, Lipscomb K, Hamilton GW. Physiologic basis for assessing critical coronary stenosis. Instantaneous flow response and regional distribution during coronary hyperemia as measures of coronary flow reserve. *Am J Cardiol* 1974;33:87–94.
24. Gerry JL, Becker LC, Flaherty JT, Weisfeldt ML. Evidence for flow-independent contribution to the phenomenon of thallium redistribution. *Am J Cardiol* 1980;45:58–62.
25. Gewirtz H, O'Keefe DD, Pohost GM, Strauss HW, McIlduff JB, Daggett WM. The effect of ischemia on thallium-201 clearance from the myocardium. *Circulation* 1978;58:215–219.
26. Grunwald AM, Watson DD, Holzgrefe HH, Irving JF, Beller GA. Myocardial thallium-201 kinetics in normal and ischemic myocardium. *Circulation* 1981;64:610–618.
27. Wilson RA, Okada RD, Struass HW, Pohost GM. Effect of glucose-insulin-potassium infusion on thallium myocardial clearance. *Circulation* 1983;68:203–209.
28. Wilson RA, Okada RD, Barlai-Kovach M, Strauss HW. The effect of glucose-insulin-potassium on thallium-201 myocardial redistribution. *Int J Nucl Med Biol* 1985;12:97–101.
29. Skou JC. The effect of pH, of ATP and of modification with pyridoxal 5-phosphate on the conformational transition between the Na^+-form and K^+-ATPase. *Biochem Biophys Acta* 1982;688:369–380.
30. Hille B. *Selective permeability: independence in ionic channels of excitable membranes.* Sunderland, MA, 1984:240.
31. Brown KA, Boucher CA, Okada RD, et al. Prognostic value of exercise thallium-201 imaging in patients presenting for evaluation of chest pain. *J Am Coll Cardiol* 1983;1:994–1001.
32. Iskandrian AS, Hakki A-H, Kane-Marsch S. Prognostic implications of exercise thallium-201 scintigraphy in patients with suspected or known coronary artery disease. *Am Heart J* 1985;110:135–143.
33. Ladenheim ML, Pollock BH, Rozanski A, et al. Extent and severity of myocardial hypoperfusion as orthogonal parameters of prognosis in patients with suspected coronary artery disease. *J Am Coll Cardiol* 1986;7:464–471.
34. Gibson RS, Watson DD, Craddock GB, et al. Prediction of cardiac events after uncomplicated myocardial infarction: a prospective study comparing predischarge exercise thallium-201 scintigraphy and coronary angiography. *Circulation* 1983;68:321–336.
35. Leppo J, O'Brien J, Rothendler JA, Getchell JD, Lee VW. Dipyridamole-thallium-201 scintigraphy in the prediction of future cardiac events after myocardial infarction. *N Engl J Med* 1984;310:1014–1018.
36. Boucher CA, Brewster DC, Darling RC, Okada RD, Strauss HW, Pohost GM. Determination of cardiac risk by dipyridamole-thallium imaging before peripheral vascular surgey. *N Engl J Med* 1985;312:389–394.
37. Leppo J, Plaja J, Gionet M, Tumolo J, Paraskos JA, Cutler

BS. Noninvasive evaluation of cardiac risk before vascular surgery. *J Am Coll Cardiol* 1987;9:269–276.
38. Staniloff HM, Forrester JS, Berman DS, Swan HJC. Prediction of death, myocardial infarction, and worsening chest pain using thallium scintigraphy and exercise electrocardiography. *J Nucl Med* 1986;27:1842–1848.
39. Kaul S, Finkelstein DM, Homma S, Leavitt M, Okada RD, Boucher CA. Superiority of quantitative exercise thallium-201 variables in determining long-term prognosis in ambulatory patients with chest pain: a comparison with cardiac catheterization. *J Am Coll Cardiol* 1988;12:25–34.
40. Stuckey TD, Burwell LR, Nygaard TW, Gibson RS, Watson DD, Beller GA. Quantitative exercise thallium-201 scintigraphy for predicting angina recurrence after percutaneous transluminal coronary angioplasty. *Am J Cardiol* 1989;63:517–521.
41. Miller DD, Liu P, Strauss HW, Block PC, Okada RD, Boucher CA. Prognostic value of computer-quantitated exercise thallium imaging early after percutaneous transluminal coronary angioplasty. *J Am Coll Cardiol* 1987;10:275–283.
42. Josephson MA, Brown BG, Hecht HS, Hopkins J, Pierce CD, Petersen RB. Noninvasive detection and localization of coronary stenoses in patients: comparison of resting dipyridamole and exercise thallium-201 myocardial perfusion imaging. *Am Heart J* 1982;103:1008.
43. Ryan TJ, Faxon DP, Gunnar RM, et al. Guidelines for percutaneous transluminal coronary angioplasty. *Circulation* 1988;78:486–502.
44. Rees G, Bristow JD, Kremkau EL, et al. Influence of aorto-coronary bypass surgery on left ventricular performance. *N Engl J Med* 1971;284:1116–1120.
45. Helfant RH, Pine R, Meister SG, Feldman MS, Trout RG, Banka VS. Nitroglycerin to unmask reversible asynergy. *Circulation* 1974;50:108–113.
46. Popio KA, Gorlin R, Bechtel D, Levine JA. Postextrasystolic potentiation as a predictor of potential myocardial viability: preoperative analyses compared with studies after coronary bypass surgery. *Am J Cardiol* 1977;39:944–953.
47. Zir LM, Dinsmore R, Vexeridis M, Singh JB, Harthorne JW, Daggett WM. Effects of coronary bypass grafting on resting left ventricular contraction in patients studied 1 to 2 years after operation. *Am J Cardiol* 1979;44:601–606.
48. Rozanski A, Berman DS, Gray R, et al. Use of thallium-201 redistribution scintigraphy in preoperative differentiation of reversible and nonreversible myocardial asynergy. 1981;64:936–944.
49. Fintel DJ, Links JM, Brinker JA, Frank TL, Parker M, Becker LC. Improved diagnostic performance of exercise thallium-201 single photon emission tomography over planar imaging in the diagnosis of coronary artery disease: a receiver-operating characteristic analysis. *J Am Coll Cardiol* 1989;13:600–612.
50. Kirsch CM, Doliwa R, Buell U, Roedler D. Detection of severe coronary heart disease with Tl-201: comparison of resting single-photon emission tomography with invasive arteriography. *J Nucl Med* 1983;24:761–767.
51. Tamaki N, Yonekura Y, Mukai T, et al. Segmental analysis of stress thallium myocardial emission tomography for localization of coronary artery disease. *Eur J Nucl Med* 1984;9:99–105.
52. Nohara R, Kambara H, Suzuki Y, et al. Stress scintigraphy using single-photon emission computed tomography (SPECT) in the evaluation of ischemic heart disease. *Am J Cardiol* 1984;53:1250–1254.
53. Tamaki N, Yonekura Y, Mukai T, et al. Stress thallium-201 transaxial emission computed tomography: quantitative versus qualitative analysis for evaluation of coronary artery disease. *J Am Coll Cardiol* 1984;4:1213–1221.
54. Brown BG, Bolson EL, Dodge HT. Quantitative computer techniques for analyzing coronary arteriograms. *Prog Cardiovasc Dis* 1986;28:403–418.

EDITORIAL
Thallium-201-Chloride for the Detection of Viable Myocardium

Although thallium-201-chloride has been widely used for the detection of myocardial ischemia/infarction, the utilization of this agent for the definition of viable myocardium is a more recent, and somewhat controversial, application. That thallium uptake might serve as a clinical marker of viability is perhaps not surprising—this monovalent cation is dependent upon the Na^+-K^+ ATPase system to achieve myocardial accumulation (*1–3*). Previous studies using the fetal mouse heart organ culture model have demonstrated that thallium uptake is reduced only when irreversible cell injury has occurred (*2,4*). At a more practical level, the "coupling" of myocardial perfusion and contraction in most clinical circumstances would in fact predict that regional thallium uptake is indicative of regional myocardial viability.

Initially applied in patients using a "dual-injection" technique, the work of Pohost and colleagues at the Massachusetts General Hospital (*5*) defined the practice of "stress-redistribution" thallium imaging, an approach that became the convention for coronary artery disease (CAD) detection. While it has become accepted that the presence of thallium redistribution is indicative of myocardial viability, it has become equally clear that a "fixed" thallium perfusion abnormality is not invariably predictive of the presence of myocardial "scar." Of particular relevance are those studies that have demonstrated resolution of such apparently "fixed" defects after coronary angioplasty or bypass surgery (*6,7*) and those that have documented preserved "metabolic function" in myocardial segments

Received Dec. 7, 1990; accepted Dec. 7, 1990.
For reprints contact: Thomas P. Rocco, MD, Clinical Associate in Medicine, Massachusetts General Hospital, Bldg. 149, 13th St., Charlestown, MA 02129.